

## PREPARATION AND CHARACTERIZATION OF POLYCAPROLACTONE MICROPARTICLES LOADING CERIUM(III) NITRATE

Lai Thu Hue<sup>1</sup> and Nguyen Thuy Chinh<sup>2,\*</sup>

<sup>1</sup>*Vietnam Department of Geology and Minerals, Hanoi, Vietnam*

<sup>2</sup>*Institute of Materials Science, Vietnam Academy of Science and Technology,  
Hanoi, Vietnam*

\*Corresponding author: Nguyen Thuy Chinh, email: [ntchinh@ims.vast.vn](mailto:ntchinh@ims.vast.vn)

Received March 25, 2026. Revised April 28, 2026. Accepted June 30, 2026.

**Abstract.** This study reports the fabrication of cerium(III) nitrate-loaded polycaprolactone (PCL) microparticles via a water-in-oil-in-water (W/O/W) double emulsion method, utilizing *Sapindus saponaria* L. extract as a natural, eco-friendly surfactant. The salt-to-polymer ratio significantly influenced the encapsulation process, with the PC75 formulation achieving an optimal encapsulation efficiency of 26.83%. Dynamic light scattering and zeta potential measurements showed that the microparticles (PC50 and PC75) possessed nanoscale dimensions (280–310 nm) and high colloidal stability (zeta potential < -30 mV). FESEM and EDX characterizations revealed a spherical morphology with a core-shell architecture, while FTIR and XRD analyses verified that the cerium nitrate was successfully embedded within the PCL matrix without altering the polymer's semicrystalline structure. These results demonstrate that the synthesized PCL microparticles, stabilized by a plant-derived surfactant, serve as promising candidates for the development of sustainable, controlled-release additives in anti-corrosion coating applications.

**Keywords:** polycaprolactone, cerium (III) inhibitor, microparticles

### 1. Introduction

Recently, research into the use of inhibitor-loaded microparticles in protective coatings has become a significant trend, particularly in the field of corrosion protection [1], [2]. Instead of using traditional corrosion inhibitors that can be toxic or have only short-term effects, microparticles capable of releasing inhibitors in a controlled manner have been developed. Microparticles containing corrosion inhibitors act as a passive barrier, and they actively release inhibitors when corrosive agents penetrate. When water or chloride ions enter the coating and come into contact with the microparticles, they trigger the release of inhibitors. The released inhibitors then travel to damaged areas of the coating,

forming a new protective film on the metal surface. This helps to "self-repair" small cracks and scratches, preventing the spread of corrosion. Among biopolymers used as carriers, polycaprolactone (PCL) is a biodegradable polyester that has been widely used in microparticle systems [1], [3]. PCL is highly biodegradable, and its degradation time depends on factors such as humidity, temperature, and pH [4]. It has been applied in the corrosion protection field [5]-[8].

The microemulsion technique is one of the common methods for fabricating polymer-based microparticles, including PCL microparticles. For instance, PCL microspheres were fabricated by double emulsion (water/oil/water), in which poly(vinyl alcohol) (PVA) was used as a stabilizer. The first water phase was added to the oil phase containing PCL in DCM and homogenized before adding the second water phase [9]. Cheng-Tang Pan *et al.* fabricated PCL microparticles by controlling particle size and uniformity through emulsification. The oil phase contained approximately 18.18% PCL, while the water phase contained approximately 13.02% PVA, and they were mixed together by vigorous stirring. The emulsion system containing PCL microparticles achieved an efficiency of approximately 87.9% with spherical particles ranging in size from 10 to 20  $\mu\text{m}$ . The microparticles had a nearly hydrophobic structure with a contact angle value of  $83.75^\circ$  [3]. PCL microspheres were also fabricated by the microemulsion method using PVA and hydroxypropyl methylcellulose as emulsifiers for insulin drug delivery. The obtained microspheres were spherical in shape, with a size of 28-43  $\mu\text{m}$  [10]. PCL microparticles containing  $\text{Ce}(\text{NO}_3)_3$  were successfully synthesized by the water-in-oil-in-water double emulsion method [1]. The emulsifier used was polyvinyl alcohol, and the solvent for dissolving PCL was DCM. After synthesizing the emulsion system, centrifugation was used to separate the microparticles, followed by freezing in a refrigerator and freeze-drying for 24 hours. Optimizing stirring speed and mixing temperature is crucial for controlling microparticle size. Under optimal conditions (stirring speed of 1000 rpm and temperature of  $50^\circ\text{C}$ ), the average size of  $\text{Ce}(\text{NO}_3)_3$ -containing PCL microparticles was 5.48  $\mu\text{m}$ . The average  $\text{Ce}(\text{NO}_3)_3$  loading capacity of these microparticles was approximately 6.15% by weight. This concentration was considered sufficient for effective  $\text{Ce}(\text{NO}_3)_3$  activity. Experimental results showed that Ce could be released from the microparticles upon immersion in an electrolyte solution (NaCl), with the release rate increasing rapidly over time and reaching saturation after 4 days of immersion.

It can be seen that the trend of using environmentally friendly corrosion inhibitors to replace toxic and carcinogenic corrosion inhibitors, such as chromium-based inhibitors, is of great interest in research and development. Although there have been studies on PCL microparticles carrying the  $\text{Ce}(\text{NO}_3)_3$  inhibitor, the use of *Sapindus saponaria* L. extract as a natural surfactant in the preparation of PCL microparticles loaded with  $\text{Ce}(\text{NO}_3)_3$  inhibitor is still limited in the literature. Therefore, this study focuses on the fabrication of anti-corrosion additives based on PCL carrying the  $\text{Ce}(\text{NO}_3)_3$  inhibitor and evaluating the characteristics, properties, and structural morphology of these formulations. The surfactants and co-surfactants, including *Sapindus saponaria* L. extract, poly(ethylene oxide) (PEO), poly(ethylene glycol) (PEG), poly(vinyl pyrrolidone) (PVP), and Tween 80, have been combined in microparticle processing.

## 2. Experiments

### 2.1. Materials

The materials and chemicals used in this study include polycaprolactone (PCL,  $M_n$  80000, Thermo Fisher Scientific, USA), cerium nitrate hexahydrate (99%, China), ethanol (99.5%, China), polyethylene oxide (PEO,  $M_n$  400000, China), polyethylene glycol (PEG,  $M_n$  400, China), polyvinylpyrrolidone (PVP, China), Tween 80 (China), and dichloromethane (DCM, 99.5%, China).

### 2.2. Preparation of *Sapindus saponaria* L. extract

First, dried *Sapindus saponaria* L. fruit (Dak Lak, Vietnam) (2 g) was chopped and added to a beaker, followed by the addition of absolute ethanol (20 mL). The mixture was stirred at 60 °C for 2 hours and filtered to obtain the *Sapindus saponaria* L. extract.

### 2.3. Preparation of PCL microparticles loaded with cerium nitrate (PCx)

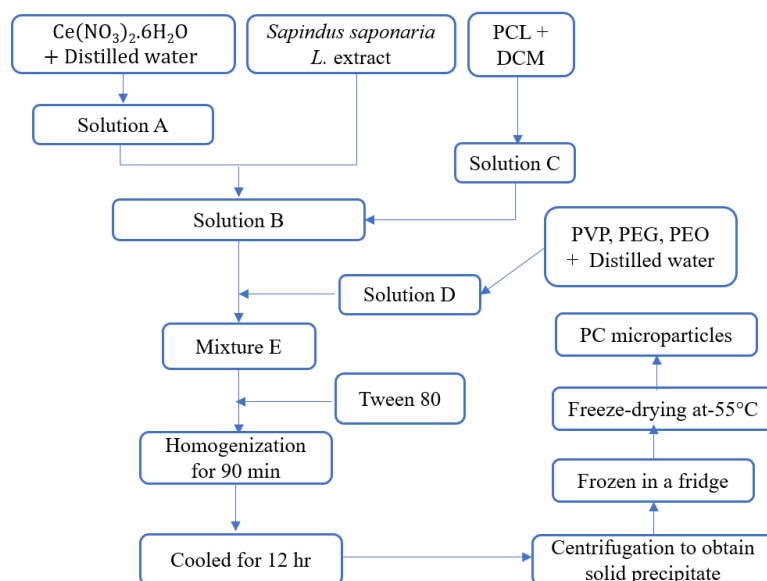


**Figure 1. Scheme of the preparation of the PC microparticles**

Initially,  $\text{Ce}(\text{NO}_3)_3 \cdot 6\text{H}_2\text{O}$  (1.3 g) was dissolved in distilled water (50 mL) using magnetic stirring and ultrasonic vibration for 30 minutes to form solution A. Subsequently, the *Sapindus saponaria* L. extract (5 mL) was added to solution A to create solution B. In a separate step, PCL (2.0 g) was dissolved in DCM (20 mL) under continuous stirring at 45 °C for 30 minutes, yielding solution C. Next, Solution C was slowly added to solution B. The resulting mixture was stirred for 1 hour and then vortexed for 10 minutes to form mixture C. Meanwhile, PEO (1.0 g), PEG (1.0 g), and PVP (3.0 g) were dissolved in distilled water (60 mL) at 90 °C. After complete dissolution, the stirring was continued for 30 minutes until the solution cooled to 50 °C, forming solution D. Following this, solution D was slowly introduced into mixture C. This combined mixture was sonicated for 30 minutes and then stirred for 1 hour to produce mixture E. Afterward, Tween 80 (2.5 mL) was added to mixture E, and the mixture was stirred and homogenized for 90 minutes. The homogenized mixture was then cooled for 12 hours, followed by

centrifugation to collect the solid fraction. Once obtained, the solid precipitate was washed 2-3 times with a distilled water/ethanol mixture (70/30, v/v) and frozen in a fridge to freeze-dry at  $-55\text{ }^{\circ}\text{C}$ . Finally, the dried product was finely ground using an agate mortar, weighed, and stored as PCL/Ce(NO<sub>3</sub>)<sub>3</sub> microparticles. Other Ce(NO<sub>3</sub>)<sub>3</sub>-PCL samples with weight ratios of 3:4, 1:1, and 4:3 were processed using a similar procedure as described above. Based on their Ce(NO<sub>3</sub>)<sub>3</sub> to PCL ratios of 1:2, 3:4, 1:1, and 4:3, the respective samples were designated as PC50, PC75, PC100, and PC125. Figure 1 presents the scheme of the preparation of the PC microparticles.

### 3. Characterization

The infrared (IR) spectra of the PC<sub>x</sub> samples were recorded using a Nicolet iS10 spectrometer (USA) at room temperature in the wavenumber range of 400 - 4000 cm<sup>-1</sup>, with 16 scans and a resolution of 8 cm<sup>-1</sup>. To measure the particle size distribution, the PC<sub>x</sub> microparticle samples were dispersed in distilled water or xylene using a TPC-15H ultrasonic vibrator (operating at a frequency of 30 kHz and a power of 150 W). The determination of particle size distribution and average particle size was carried out on a Horiba SZ-100Z2 nanoparticle size and Zeta potential analyzer (Horiba, Japan). Field emission scanning electron microscopy (FESEM) images of the PC<sub>x</sub> microparticle samples were captured using an S4800 FESEM system (Hitachi, Japan). Energy-dispersive X-ray spectroscopy (EDX) spectra of the samples were recorded using a Horiba 7593-H detector (Kyoto, Japan) integrated into the S4800 FESEM system. X-ray diffraction (XRD) patterns of the samples were recorded on a D8-Advance diffractometer (Bruker, Germany). The analysis was performed using CuK $\alpha$  radiation with a step size of 0.01° to 0.02° in the 2 $\theta$  scanning range from 10° to 70°. The loading efficiency of microparticles was determined as follows: 0.01 g of microparticles was dispersed in 10 mL of distilled water, and the mixture was stirred on a magnetic stirrer for 6 hours before centrifuging to obtain the solution. The solution was measured on an Ultraviolet-visible (UV-Vis) Libra S80 (Biochrom, UK). The loading efficiency of microparticles was calculated based on UV-Vis data and through a calibration equation ( $y = 39072x + 0.7257$ ,  $R^2 = 0.9117$ ,  $\lambda_{\text{max}} = 239\text{ nm}$ ).

## 4. Results and discussion

### 4.1. Macroscopic images and loading efficacy of PC<sub>x</sub> microparticles

The macroscopic images of the PC<sub>x</sub> microparticle samples in Figure 2 show that the products were obtained in the form of a fine, uniform white powder. The net weights of the PC50, PC75, PC100, and PC125 samples were 1.9260 g, 2.1995 g, 1.6837 g, and 1.8347 g, respectively. Consequently, the production yields, calculated based on the total initial weight of PCL and Ce(NO<sub>3</sub>)<sub>3</sub>·6H<sub>2</sub>O, reached 57.80%, 55.02%, 36.08%, and 34.42%, respectively. These values indicate a moderate production yield. The loss of mass is due to the centrifugation and washing process of the sample and the excess material that does not emulsify. As the initial weight of the Ce(III) salt increased, the production yield exhibited a decreasing trend. This is likely due to the loading capacity of the PCL matrix reaching saturation at a low Ce(III) salt content (50-75 %).

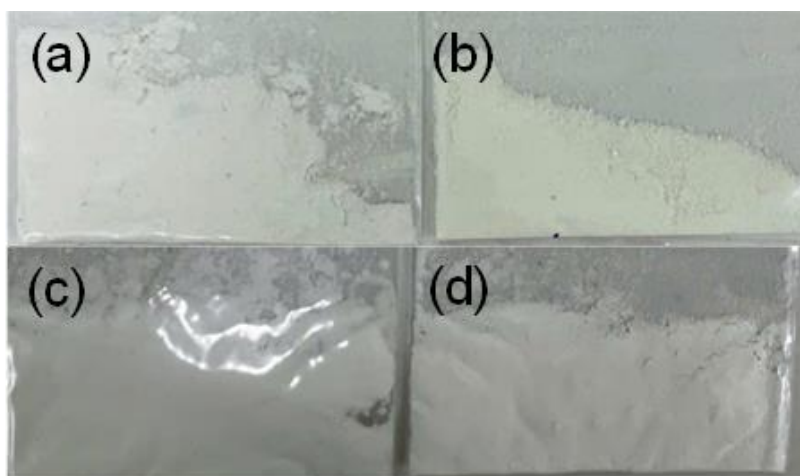


**Figure 2. Macroscopy images of PC50 (a), PC75 (b), PC100 (c) and PC125 (d)**

To evaluate the loading efficiency of the PC microparticles, UV-Vis spectroscopy was employed. The results showed that the loading efficiency values for PC50, PC75, PC100, and PC125 were 15.63%, 26.83%, 16.46%, and 16.52%, respectively. These findings indicate that the optimal loading capacity was achieved at a 75% salt-to-polymer ratio, suggesting that this concentration represents the saturation point for Ce(III) nitrate within the PCL matrix under the investigated conditions.

#### **4.2. IR spectra of PCx microparticles**

Figure 3 presents the IR spectra of the  $\text{Ce}(\text{NO}_3)_3 \cdot 6\text{H}_2\text{O}$  salt, PCL, and the PCx microparticles at ratios of 1:2, 3:4, 1:1, and 4:3. Observing the IR spectrum of the Ce(III) salt reveals its characteristic peaks. Specifically, a broad peak appears at  $3383\text{ cm}^{-1}$ , which is characteristic of the stretching vibration of the -OH group. It is likely to have originated from the water of crystallization within the salt or absorbed moisture. Additionally, the peak at  $1632\text{ cm}^{-1}$  is associated with the bending vibration of water molecules. The peaks in the  $1436\text{ cm}^{-1}$  and  $1294\text{ cm}^{-1}$  regions represent the characteristic vibrations of the salt's molecular framework [11]. In the spectra of the PCx microparticle samples, the simultaneous appearance of the characteristic peaks of PCL (at  $1721\text{ cm}^{-1}$  and  $2942\text{ cm}^{-1}$ ) and the weaker peaks of the Ce(III) salt can be observed. This confirms that the Ce salt was successfully encapsulated within the PCL microparticle structure. The position of the PCL carbonyl peak remained unchanged at  $1721\text{ cm}^{-1}$  [1], [10] across all microparticle samples, indicating that the chemical structure of the PCL polymer backbone was not altered in the presence of the Ce(III) salt.

Furthermore, the broad peak at  $3383\text{ cm}^{-1}$  of the Ce(III) salt either disappeared or exhibited a significantly reduced intensity in the microparticle samples. This is likely due to the Ce(III) salt being deeply encapsulated within the hydrophobic PCL polymer shell, thereby restricting the exposure of free hydroxyl groups or surface water. As the Ce(III) salt ratio increased (from 1:2 to 4:3), its characteristic peaks in the region below  $1500\text{ cm}^{-1}$  became slightly more distinct compared to the sample with a lower concentration, reflecting the increased salt content within the microparticles.

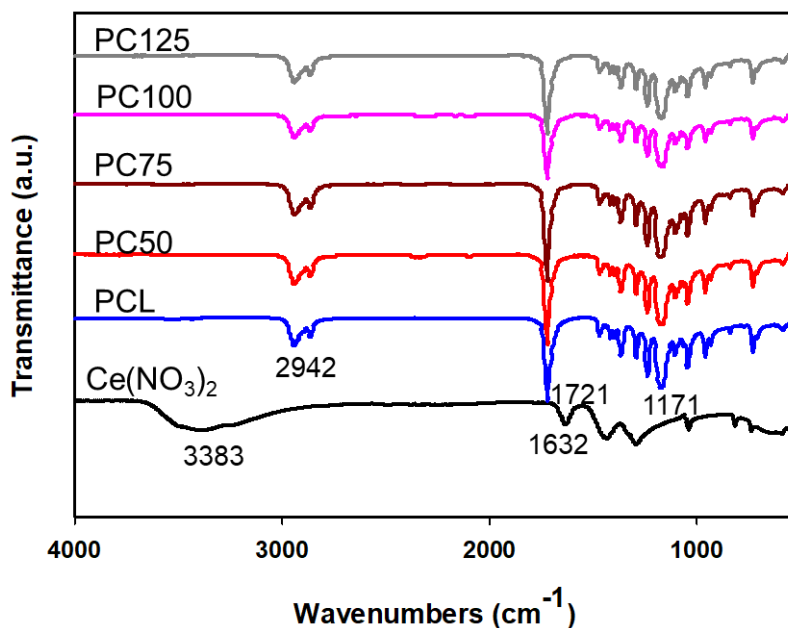


*Figure 3. IR spectra of PCx microparticle samples*

#### 4.3. Size distribution and zeta potential

The size distribution in distilled water and xylene of PCx microparticle samples is displayed in Figure 4A and Figure 4B. The results indicate that the particle size fluctuates significantly based on the ratio of PCL and Ce(III) salt and the dispersion environment. For the PCx system, the microparticles exhibited the smallest and most stable sizes at the lower loading ratios of PC50 and PC75, with average sizes in distilled water of 308.9 nm and 284.7 nm, respectively. Notably, the size distribution of the PC75 sample was highly concentrated, primarily in the narrow range of 100–200 nm (Figure 4A). However, when the ratio PCL/Ce(III) reached 1:1 (sample PC100), the average particle size abruptly increased almost tenfold to 2796.2 nm. This dramatic increase suggests that at an equimolar-like ratio or critical loading threshold, the encapsulation efficiency is disrupted, leading to the aggregation or swelling of the polymer matrix due to the excessive hydrophilic nature of the incorporated  $\text{Ce}(\text{NO}_3)_3$  salt. Interestingly, further increasing the salt content in the PC125 sample resulted in a size reduction to 1404 nm (Figure 4C), though it remained significantly larger than those of the low-ratio samples. A similar trend in particle size variation was also observed when the microparticles were dispersed in xylene, although the sizes were generally larger than those in distilled water, possibly due to the swelling behavior of PCL in organic solvents (Figure 4B). The great distribution in xylene solvent is an advantage for its application as a promising anti-corrosion additive for organic coatings such as epoxy resins.

Figure 4D shows the zeta potential results for the PCx microparticle systems. All samples exhibited negative zeta potential values, indicating that the surfaces of the microparticles are negatively charged. This negative charge generates electrostatic repulsion between the particles, effectively preventing agglomeration. Most of the samples (PC50, PC75, and PC125) possessed absolute zeta potential values ranging from

[36.2] to [39.7] mV. According to standard colloidal science criteria, systems with an absolute zeta potential greater than 30 mV ( $|Z| > 30$  mV) are considered to have excellent electrostatic stability [12], [13]. The only exception was the PC100 sample, which showed a significantly lower absolute zeta potential (-14.2 mV). This reduction in surface charge corresponds directly with the massive increase in particle size observed for this sample, confirming that the diminished electrostatic repulsion allowed severe particle aggregation to occur.

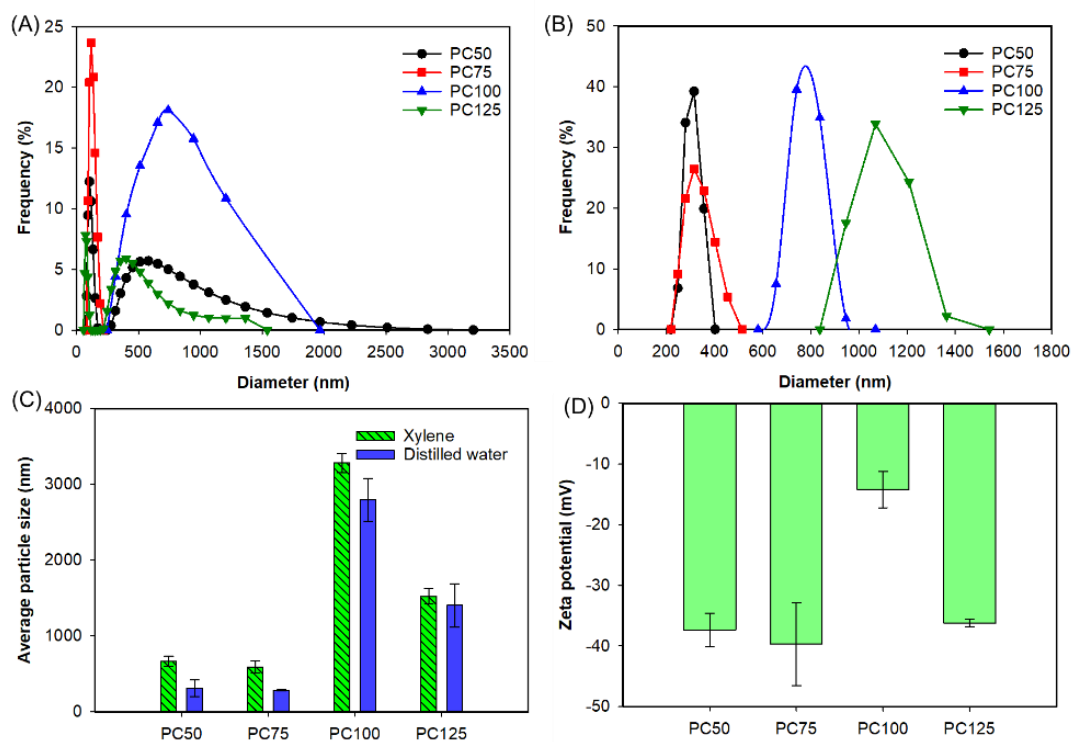


**Figure 4.** Size distribution in distilled water (A), size distribution in xylene (B), average particle size in xylene and distilled water (C), and zeta potential (D) of the PCx microparticle samples

#### 4.4. Morphology and element composition

As shown in Figure 5, the PC75 microparticle exhibits an irregular spherical morphology with a rough, uneven structure distributed across the polymer matrix. Among the synthesized formulations, this sample presents the most complex surface topography, characterized by the presence of numerous micropores. Scientifically, the formation of these porous structures can be primarily attributed to the rapid evaporation rate of the volatile organic solvent, such as dichloromethane, during the microparticle solidification process. Furthermore, osmotic pressure differences between the internal and external aqueous phases in the double emulsion system, combined with strong physicochemical interactions between the hydrophilic Ce(III) salt inhibitor and the hydrophobic PCL backbone, likely contribute to localized phase separation and the resulting surface invaginations.

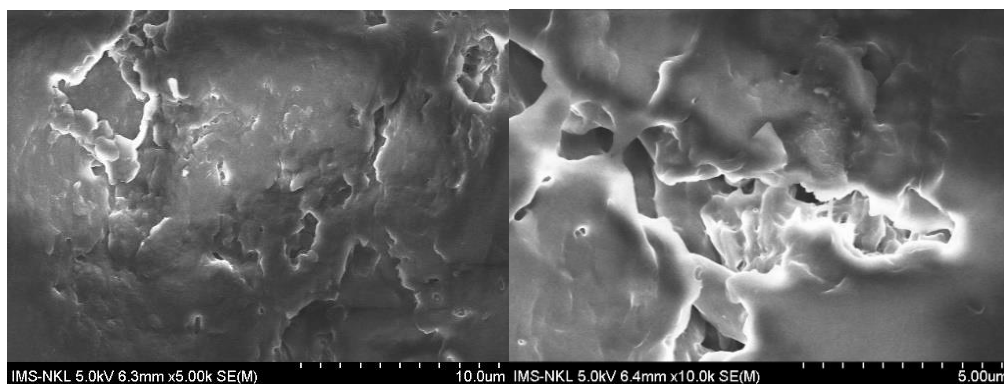


**Figure 5. FESEM images of the PC75 microparticle sample**

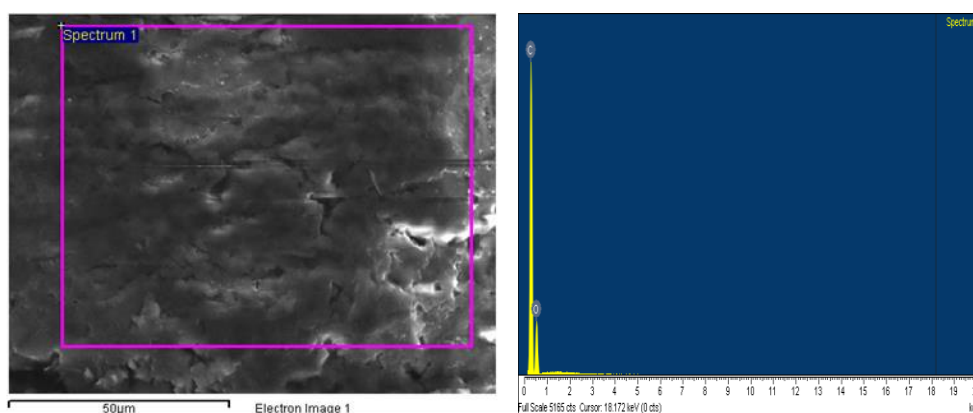


**Figure 6. SEM-EDX spectrum of PC75 microparticle sample**

The EDX analysis results presented in Figure 6 reveal that the elemental composition of the PC75 microparticle surfaces consists exclusively of carbon (C) and oxygen (O). Because EDX is a surface-sensitive technique, the complete absence of characteristic elemental signals from the respective Ce(III) salt inhibitor on the surface provides compelling evidence that the active agents are successfully and deeply encapsulated within the core of the microparticles. In this configuration, the PCL matrix acts effectively as a thick, protective outer shell. Specifically, the elemental analysis indicates that the PC75 sample comprises 66.06% C and 33.94% O. These carbon-to-oxygen ratios are highly consistent with the theoretical stoichiometric composition of pure polycaprolactone, further confirming the absence of surface-adsorbed inhibitors and the high efficiency of the core-shell encapsulation process.

#### 4.5. XRD pattern

Figure 7 presents the XRD pattern of the PC75 microparticle sample. The diffractogram of the neat PCL exhibits two sharp, high-intensity diffraction peaks at  $2\theta$  angles of approximately  $21.4^\circ$  and  $23.8^\circ$ . These two peaks correspond to the (110) and (200) crystallographic planes of the orthorhombic crystal structure of PCL, respectively [14], [15]. This confirms the highly semi-crystalline nature of the PCL polymer.

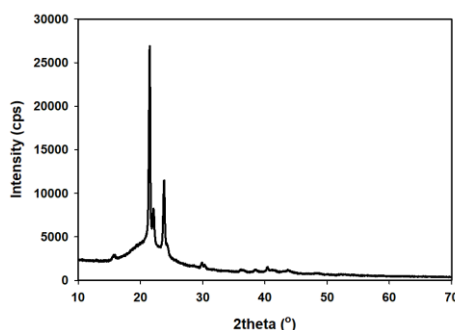


**Figure 7. XRD pattern of PC75 microparticle sample**

Regarding the synthesized microparticles, the XRD patterns of the encapsulated systems reveal that the characteristic diffraction peaks of PCL at  $21.4^\circ$  and  $23.8^\circ$  are perfectly preserved. The positions of these peaks remain unchanged, indicating that the crystalline domains of the PCL matrix were not significantly disrupted or altered during the encapsulation process. Crucially, the characteristic diffraction peaks of the loaded Ce(III) salt are virtually absent in the microparticle spectra. This observation can be scientifically explained by two main factors. First, it strongly suggests that the salts are deeply and completely encapsulated within the core of the PCL matrix, where the thick polymer shell masks their signals, corroborating the findings from the earlier FESEM and EDX analyses. Second, it implies that the incorporated inorganic salts may exist in an amorphous state or be molecularly dispersed within the amorphous regions of the polymer network rather than forming large crystalline aggregates, thus yielding no distinct crystalline diffraction signals.

## 5. Conclusions

This study successfully demonstrated the fabrication of potential anti-corrosion microparticles by encapsulating the eco-friendly  $\text{Ce}(\text{NO}_3)_3$  inhibitor within a biodegradable polycaprolactone (PCL) matrix. The use of *Sapindus saponaria* L. extract as a natural surfactant in the double emulsion process proved to be a highly effective and green approach. The physicochemical characterizations confirmed that the initial salt-to-polymer loading ratio strictly governs the particle size and colloidal stability. The PC50 and PC75 ratios emerged as the optimal formulations, yielding uniformly distributed nanoparticles with high electrostatic stability, preventing unwanted agglomeration. Comprehensive structural analyses, including FESEM, EDX, FTIR, and XRD, convergently verified the successful core-shell architecture of the microparticles. The PCL matrix effectively acted as a robust protective shell, deeply encapsulating the amorphous Ce(III) salt without altering the polymer's inherent semi-crystalline framework or chemical backbone. Although direct corrosion performance was not evaluated in this stage, the obtained structural characteristics and stability suggest that these Ce-loaded PCL microparticles are promising candidates for controlled-release applications. This research provides a foundation for developing environmentally compatible additives for future self-healing organic coatings aimed at enhancing corrosion protection.

**Note for contributor:**

- Short bio: Lai Thu Hue is a researcher at the Geological Analysis and Verification Center, Vietnam Department of Geology and Minerals, Vietnam; Nguyen Thuy Chinh is an Associate Professor, Senior Researcher at the Institute of Materials Science, Vietnam Academy of Science and Technology, Vietnam.

- Author's contributions: Lai Thu Hue: data analysis, visualization, writing; Nguyen Thuy Chinh: conceptualization, funding acquisition, writing, review & editing, formal analysis, supervision, data curation, resources, investigation, methodology.

**Conflict of interest.** The authors declare no competing interests

**Acknowledgments.** This research is funded by the Vietnam National Foundation for Science and Technology Development (NAFOSTED) under grant number NCU02-2024.12.

## REFERENCES

- [1] P. Thiangpak & A. Rodchanarowan, "The synthesis of polycaprolactone (PCL) microspheres containing cerium (III) nitrate ( $\text{Ce}(\text{NO}_3)_3$ ) self-healing agent via double emulsion evaporation method", *Materials Today Communications*, vol. 25, pp. 101668, 2020. DOI: 10.1016/j.mtcomm.2020.101668
- [2] R. Raj, Y. Morozov, L. M. Calado, M. G. Taryba, R. Kahraman, A. Shakoob & M. F. Montemor, "Inhibitor loaded calcium carbonate microparticles for corrosion protection of epoxy-coated carbon steel", *Electrochimica Acta*, vol. 319, pp. 801-812, 2019. DOI: 10.1016/j.electacta.2019.07.059
- [3] C. T. Pan, Y. M. Hwang, Y. M. Lin, S. W. Zeng, S. Y. Wang, S. W. Kuo, S. P. Ju, S. S. Liang, Z. H. Liu & C. K. Yen, "Development of polycaprolactone microspheres with controllable and uniform particle size by uniform design experiment in emulsion progress", *Sensors and Materials*, vol. 31, no. 2, pp. 311-318, 2019.
- [4] M. A. Ntrivala, A. C. Pitsavas, K. Lazaridou, Z. Baziakou, D. Karavasili, M. Papadimitriou, C. Ntagkopoulou, E. Balla & D. N. Bikiaris, "Polycaprolactone (PCL): the biodegradable polyester shaping the future of materials – a review on synthesis, properties, biodegradation, applications and future perspectives", *European Polymer Journal*, vol. 234, pp. 114033, 2025. DOI: 10.1016/j.eurpolymj.2025.114033
- [5] Y. Xu, T. Wang, X. Qu, Z. Liu, Y. Guo, G. Li, Z. Zhang, J. Lian & L. Ren, "Preparation of anticorrosion, biocompatible and antibacterial dicalcium phosphate dihydrate/polycaprolactone-titania composite coating on Mg alloy", *Progress in Organic Coatings*, vol. 172, pp. 107133, 2022. DOI: 10.1016/j.porgcoat.2022.107133
- [6] H. M. Mousa, M. A. Mahmoud, A. S. Yasin & I. M. A. Mohamed, "Polycaprolactone tridentate ligand corrosion inhibitors coated on biodegradable Mg implant", *Journal of Coatings Technology and Research*, vol. 18, pp. 1191-1197, 2021. <https://doi.org/10.1007/s11998-021-00478-w>

- [7] K. Berdimuradov, E. Berdimurodov, A. Kumar, O. Dagdag, M. Rbaa & B. Jain, “Chapter 8: Biodegradable synthetic polymers as aqueous corrosion inhibitors: Past and present advancements and future prospects” in *Polymers as Corrosion Inhibitors: Principles to Applications*, C. Verma, Ed. UK: Royal Society of Chemistry, 2025, vol. 41, pp. 139-156. DOI: 10.1039/9781837677214-00139
- [8] K. Rajitha & K. N. Mohana, “Application of modified graphene oxide – Polycaprolactone nanocomposite coating for corrosion control of mild steel in saline medium”, *Materials Chemistry and Physics*, vol. 241, pp. 122050, 2020. DOI: 10.1016/j.matchemphys.2019.122050
- [9] D. Ibraheem, M. Iqbal, G. Agusti, H. Fessi & A. Elaissari, “Effects of process parameters on the colloidal properties of polycaprolactone microparticles prepared by double emulsion like process”, *Colloids and Surfaces A: Physicochemical and Engineering Aspects*, vol. 445, pp. 79-91, 2014.
- [10] A. Mukerjee, V. Pruthi & V. R. Sinha, “Preparation and characterization of poly-ε-caprolactone carrier particles for controlled insulin delivery”, *2006 International Conference on Biomedical and Pharmaceutical Engineering*, IEEE, pp. 276-279, 2006. DOI: 10.1109/ICBPE.2006.348599
- [11] W. Wattanathana, N. Suetrong, P. Kongsamai, K. Chansaenpak, N. Chuanopparat, Y. Hanlumyuang, P. Kanjanaboos & S. Wannapaiboon, “Crystallographic and spectroscopic investigations on oxidative coordination in the heteroleptic mononuclear complex of cerium and benzoxazine dimer”, *Molecules*, vol. 26, no. 17, pp. 5410, 2021. DOI: 10.3390/molecules26175410
- [12] S. Mohammadi-Jam, R. W. Greenwood & K. E. Waters, “An overview of the temperature dependence of the zeta potential of aqueous suspensions”, *Results in Engineering*, vol. 27, pp. 105698, 2025. DOI: 10.1016/j.rineng.2025.105698
- [13] K. A. AlMuhaysh, A. Sergis & Y. Hardalupas, “Effects of pH and Nanoparticle Concentration on Al<sub>2</sub>O<sub>3</sub>–H<sub>2</sub>O Nanofluid Stability”, *International Journal of Thermophysics*, vol. 46, pp. 82, 2025. DOI: 10.1007/s10765-025-03557-x
- [14] Q. S. Kahdima, Z. Benzarti, M. H. Mousad, M. H. Rasheede, N. Abdelmoulab & A. Khalfallah, “Enhancing the multifunctional properties of polycaprolactone/chitosan films with zirconium dioxide nanoparticles for biomedical and flexible optoelectronic applications”, *RSC Advances*, vol. 15, pp. 31788-31805, 2025. DOI: 10.1039/D5RA05303J
- [15] S. H. Chung, S. A. Barker, D. Q. M. Craig & J. Huang, “Characterization and drug delivery potential of biodegradable PCL/PLA scaffolds fabricated via solvent-cast direct-writing”, *Macro Molecular Materials and Engineering*, vol. 310, no. 11, pp. e00119, 2025. DOI: 10.1002/mame.202500119